MICROCOPY RESOLUTION TEST CHART

NATIONAL BUREAU OF STANDARDS-1963-A

FOREIGN TECHNOLOGY DIVISION

INTERNATIONAL AVIATION
(Selected Articles)

84 05 08 042

EDITED TRANSLATION

FTD-ID(RS)T-0041-84   18 April 1984

MICROFICHE NR: FTD-84-C-000400

INTERNATIONAL AVIATION   (Selected Articles)

English pages: 17

Source: Guoji Hangkong, Nr. 237, November 1982, pp. 2-5;
         6; 23
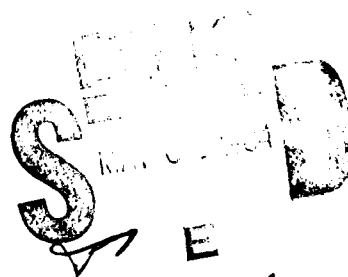
Country of origin: China
Translated by: LEO KANNER ASSOCIATES
              F33657-81-D-0264
Requester: FTD/TQTA
Approved for public release; distribution unlimited.

Accession For	
NTIS GRA&I	X
DTIC TAB	
Unannounced	☐
Justification	

A-1

THIS TRANSLATION IS A RENDITION OF THE ORIGI-NAL FOREIGN TEXT WITHOUT ANY ANALYTICAL OR EDITORIAL COMMENT. STATEMENTS OR THEORIES ADVOCATED OR IMPLIED ARE THOSE OF THE SOURCE AND DO NOT NECESSARILY REFLECT THE POSITION OR OPINION OF THE FOREIGN TECHNOLOGY DI-VISION.	PREPARED BY: TRANSLATION DIVISION FOREIGN TECHNOLOGY DIVISION WP-AFB, OHIO.

Table of Contents

GRAPHICS DISCLAIMER

All figures, graphics, tables, equations, etc. merged into this
translation were extracted from the best quality copy available.

WING-TIP SAIL TEST ON THE Y-11 AGRICULTURAL AIRCRAFT

Guan Ruizhang

In GUOJI HANGKONG [INTERNATIONAL AVIATION], Issue No. 1 (1980), tests and
research on the Y-11 agricultural aircraft with the installation of wing-tip
ailerons were introduced. Recently, based on the aforementioned research, the
author and his colleagues conducted tests of wing-tip sails, which have higher
aerodynamic efficiency than wing-tip ailerons, since they can more effectively
disperse the wing-tip vortex and reduce the induced drag of the entire aircraft.

Fundamental principle: The aerodynamic principle of wing-tip sails is
basically similar to that of wing-tip ailerons during flight of an aircraft; the
high-pressure air under the wings winds around the wing tips to flow toward the
upper surface of the wings in spirals. This creats a tail vortex and causes
induced drag. The installation of ailerons or sails at the wing tips can .restrain
this spiral flow. Thus, the streamlines are straightened, reducing the intensity
of the tail vortex and also the induced drag. However, the direction of the
stream field at the wing tip is varied; if only an aileron is installed at the
wing tip, delicate bending and torsion are required in the aerodynamic design in
order to adapt to the deflection angle of local air flow in different directions.
Otherwise, the aerodynamic efficiency is unable to be sufficiently exploited.
The installation of wing-tip sails is equivalent to the installation of multiple
ailerons at the wing tips according to different characteristics of the stream

field at different positions of the wing tip. Of course, this leads to much higher efficiency. Figure 1 is a schematic diagram of the stream field for three sails. We can see that on the one hand, the side wind is utilized to provide a push, as for sails in a sailboat; and on the other hand, like stationary fan blades, the rotating (incoming) stream at the wing tip can be "combed" into a uniform and straight airflow. In addition, the wing-tip sails can more effectively dissect the original concentrated vortex at the wing tip so that it is smaller and narrower than the vortex caused by wing-tip ailerons.
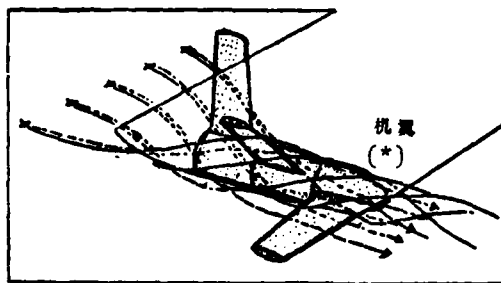
Fig. 1. The wing-tip stream field and wing-tip sails during flight of an aircraft (dotted lines indicate stream-lines of the incoming flow without installation of sails; solid lines indicate streamlines with installation of sails).
Key: (*) Aircraft wing.

Installation of sails: From Fig. 1, we can see that positions of various sails should alternate since the streamlines at the wing tip are spiral shaped. Moreover, the trend of the spirals should refer to the layout. Figure 2 is a schematic diagram of sail installation. The magnitude of the included spiral angle of two sails (front and rear) should be determined by wind tunnel tests. Since lifts are produced at various sails, the respective downward stream field is also produced. Therefore the spiral angle should be so small that a sail is situated in the downwind stream field of other sails; this will reduce the lift and increase the drag of the particular sail, besides producing too early separation of the winding flow of the sail.
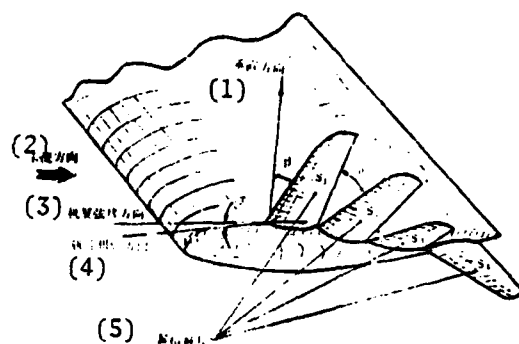
2

Fig. 2. Schematic diagram for instal-
lation of wing-tip sails.
Key: (1) Vertical direction; (2) Direc-
tion of incoming flow; (3) Chord direction
of the aircraft wing; (4) Root-chord di-
rection of a sail; (5) Wing-tip sails.

Length of sails: Figure 3 gives the measurement results abroad on the wing-tip stream field. At a given angle of attack, the ratio ϕ/α between the direction angle ϕ (of the local stream field at the wing tip) and the angle (of attack) α of the incoming flow rapidly decreases with increasing distance from the upper surface. If sails are too long, it is possible that one portion of the sails is outside the interference stream field. This not only fails to provide lift, but also increases some frictional drag. The length of a sail is primarily determined by the angle of attack of the aircraft wing. For a larger angle of attack (for example, 10°), the length is 0.41 times the chord length of the wing tip of the aircraft. For a smaller angle of attack (such as 6°), the length of sail is 0.30 times the chord length of the aircraft wing, and even as small as 0.24 (times the chord length of the wing tip) can be used.

Usually, the shape of a sail is a trapezoid with taper ratio about 0.5, and the length of the root chord is 0.16 times the chord length of the aircraft wing.
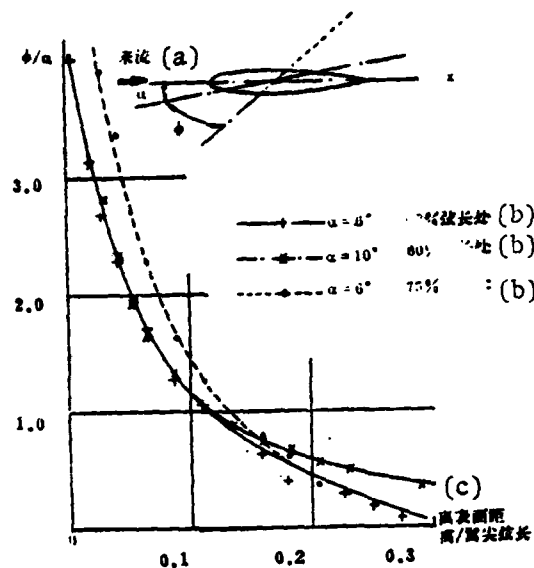
3

Fig. 3. A measurement result of the
stream field at the wing tip.
Key: (a) Incoming flow; (b) At ....
times chord length; (c) Apart from
surface distance/wing tip chord length.

Wing types of sails: Situated in a complicated interference stream field,
a sail should adopt the high-lift low-drag wing type with a wide range of lift
coefficient of low drag. The particular wing type not only can provide better
aerodynamic effect under design conditions, but also does not cause separation
of sails even under conditions unforeseen during design. For example, we can
use wing types, such as GA(W)-1, GA(W)-2 and GU; or we can use NACA6 series
symmetrical wing types, such as NACA630212. To ensure that the sails do not
separate, the curvature of the wing type close to the wing tip of the sail
should be small or, it should have no curvature at all. The closer to the wing
root the sail is, the greater is the curvature of the wing type.

Chord angle of sails: The chord angle is the included angle (refer to
in Fig. 2) between the root-chord direction of the sail and the wing-chord

4

direction of the aircraft. Actually, the chord angle determines the operational angle of attack of the sail. Since various sails are situated in different local stream fields, there are different chord angles; the chord angle toward the outside is considered positive. The chord angle of the first sail is the largest, gradually decreasing in succeeding sails. In addition, we can see from Fig. 3 that the larger the angle the closer it is to front fringe of the wing surface. Therefore, the increase of chord angle is equivalent to a decrease of local angle of attack at the connection between the sail and the aircraft wing, which does not cause root separation of the sails.

Inclination angle of a sail: The included angle β between the chord plane of a sail and the chord plane of the wing is defined as the inclination angle of the sail. In order to let a sail avoid the wake coming from other sails, with consideration of the effect of longitudinal- and lateral-direction stability of the aircraft by the sail, as well as factors of separation of the adhering layer, different β angles should be taken for different sails. Generally speaking, for the first sail, $\beta_1 = 0°$; succeeding sails have increasing magnitudes (in sequence) of the angle. The included angle between two sails is better at 15° to 20°. As indicated by tests abroad, for the same number of sails, the smaller the inclination angle of the sail, the better is the effect in reducing the induced drag.

Torsional angle of a sail: Figure 3 also indicates that the angle ϕ increases rapidly in magnitude the closer it is to the upper surface of the aircraft wing; the magnitude can attain four times the angle of attack of the incoming flow. However, at an altitude of only 0.2 times the chord length of the wing surface, angle ϕ decreases to 0.5 times the angle of attack (of the incoming flow) and even smaller. In order to ensure that the root of the sail not separate, or to increase the aerodynamic effect at the sail tip, aerodynamic torsion design should be conducted on the sail. If the cross section at the tip of the sail is considered the datum of torsion design on the lienar variation rule, and the cross section of the wing root has a negative (torsion) angle, the largest torsion angle can be -20°.

5

Number of sails: By reducing the induced drag, the number of sails should be greater for better effect. However, sails not only produce lift but also drag, including frictional resistance and induced drag. More sails can not only lead to greater frictional resistance, but also more serious interference between sails. Too many sails unavoidably lead to a situation where some sails are situated in the wake of other sails. In addition, the interference of the adhering layer leads to local separation, thus reducing the aerodynamic effect of the sails. By taking experimental results abroad as an example, when the spread-out length of a sail is 0.24 times the chord length of the aircraft wing, the drag factor rapidly decreases with increasing number of sails. The aerodynamic effect is low when the number of sails is more than three. Since the aerodynamic effect is related to the length of the sail, if the sails are relatively long, as many as four sails is allowed.

In 1978, research on wing-tip sails was conducted in the United Kingdom. For a 1:7 model of the "Paris" aircraft, low-speed wind tunnel tests were conducted on a group of sails. When $\alpha=6°$ and $C_L=0.5$, by only installing a sail at the wing tip, the induced drag of the entire aircraft can be reduced by 12 percent; by installing three sails, the induced drag can be reduced 28 percent, and the lift-to-drag ratio raised by 25 percent. Later, flight tests were conducted. As revealed by results, 9 percent of the induced drag can be reduced by installing one sail at each side of the wing. By installing three sails at each side of the wing, the induced drag can be reduced 29 percent; the aerodynamic effect is quite desirable. By comparison, the installation of wing-tip ailerons can reduce at best the induced drag by 20 to 25 percent (KC-135); for a DC-10 model aircraft, only a 12 percent reduction in induced drag is obtained. In 1979, test flights on the "Paris" MS760 aircraft proceeded for fuel consumption and maneuver tests in the United Kingdom; when three sails were installed at the wing tip and the lift coefficient was 0.22, the reduction of the induced drag was 27 percent. Owing to reduction of the overall drag, for the standard lift coefficient $C_L=0.35$, 4.5 percent fuel was saved. At $C_L=0.8$, the fuel saving was 11 percent. After aircraft takeoff, a pilot can have a faster climb rate. On increasing the number of sails, there is no variation in roll attenuation of aileron maneuver.

6

In 1981, the author and his colleagues conducted wing-tip sail tests on the Y-11 aircraft model in a 4x3 m^2 low-speed wind tunnel; the sails are trapezoidal with a taper ratio of 0.5; sail lengths of 0.41 and 0.24 times the chord length of the wing for long and short sails. The GU wing type was used for long sails; NACA0012 and CU wing types were used for short sails. The torsion angles of the sails were, respectively, 12° (long sails) and 7° (short sails). In tests, combinational selections were made on inclination angle, chord angle and number of sails installed. As revealed by the experimental results, the inclination of the lift line of the entire aircraft can be increased by 9 percent after installing four sails. With flap deflection (considering the ground effect), the maximum increase of the lift coefficient was 5 percent; the maximum lift-to-drag ratio of the aircraft was increased by 9.7 percent. For the operational lift coefficient, the reduction of induced drag was 20 percent. In addition, the experiment revealed that sails have little effect on stability in the longitudinal and lateral directions. Figures 4 and 5 show typical results of the experiment.

Fig. 4. Effect on lift characteristics of Y-11 aircraft by sails. Key: (a) Lift coefficient; (b) Entire aircraft; (c) Installation of four sails at wing tip of the aircraft; (d) Angle of attack in degrees.
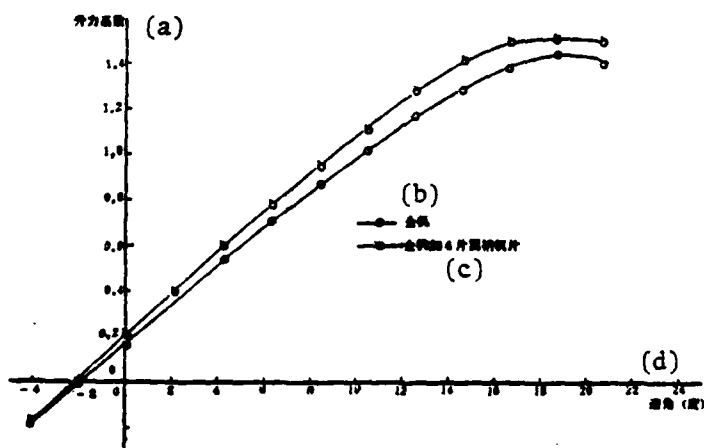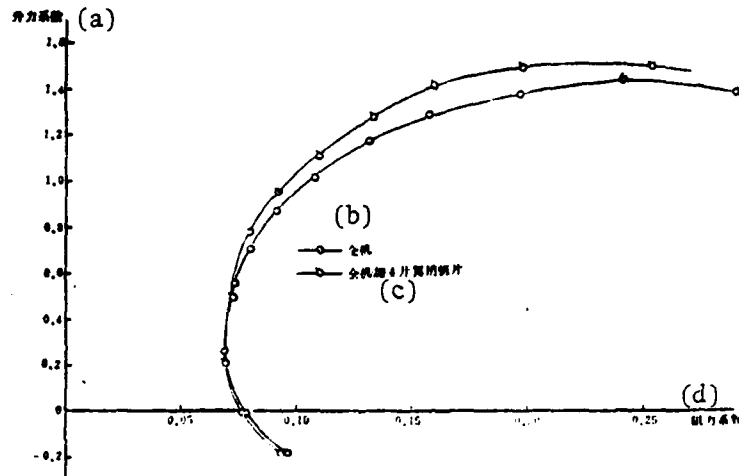
7

Fig. 5. Effect on lift and drag characteristics of Y-11
aircraft by sails.
Key: (a) Lift coefficient; (b) Entire aircraft; (c)
Installation of four sails at wing tip of the aircraft;
(d) Drag coefficient.

8

BRIEF ON AERODYNAMIC HANDBOOK FOR AVIATION (I)

Zhao Xuexun

THE HANDBOOK OF AERODYNAMICS,the first suit of complete and useful hand-book for aeronautical enginerring in China,is organized and compiled by CAE and CARDC. The hand-book is in four volumes.Vol.1 includes symbols,coodinate systems, measured units, the fundamental formulae and definitions of important parameters,etc.Vol.2 includes calculative methods of the longitudinal aerodyuamic characteristics of aircraft and design methods of aircraft components.Vol.3 includes calculative methods of the lateral and directional derivatives and some special problems. Vol.4 includes calculative methods of flight dynamics.

The major content will be introduced in two issues.

HANGKONG QIDONGLI SHOUCE [AERODYNAMIC HANDBOOK FOR AVIATION]-was sponsored, compiled and written by the China Aeronautics Research Institute and the China Aerodynamic Research and Development Center; this is a reference book for flight-vehicle design personnel, and professional staff of aeronautical engineering colleges and schools, as well as science and technology units. In the process of compilation, the staff heeded China's actual situation to seriously conclude and utilize the available experience and results in scientific research; they developed some new methods. By analysis and calculation examples of models, selections, verification and innovation were conducted on new results published abroad in the 1970s.

The handbook is divided into four volumes, containing specifications of symbols; coordinate axis systems, and measurement units; standard international atmospheric data; fundamental equations of aerodynamics and aircraft motion equations; as well as calculation methods of aerodynamic characteristics and flight performances from the (small angle of attack) linear range to the (large angle of attack) nonlinear range, from low speed to transonic speed, in the air and near the ground, in static and dynamic conditions, and for a longitudinal direction and lateral direction of aircraft without objects attached outside the fuselage.

In order to meet requirements of fast estimate of engineering design, key calculation methods are the use of analytical expression equations, and graphs and charts of systems. Moreover, considering that application of aerodynamic calculations is more and more widespread in aircraft design, ten calculation and design source programs on China's general-use computers are presented in the handbook.

The first volume (of the handbook) covering the fundamental presentation was published in 1975 by the Institute of Science and Technology Information, the Third Ministry of Machine Building. The second volume covering the calculation methods of longitudinal aerodynamic properties on an object at equilibrium will be published soon by the National Defense Industry Publishing House. The third volume covering calculation methods of lateral direction derivatives and other special problems is undergoing compilation and writing. The fourth volume covering calculations of characteristics of flight mechanics was published in 1978 by the National Defense Industry Publishing House.

Main contents of the various volumes are presented in the following:

Volume One   Fundamentals

There are three chapters in this volume. Chapter one first specifies common symbols used in aerodynamics (including flight mechanics), coordinate axis systems, and measurement units. In addition, important parameters are defined in a scientific way. In order to use data from abroad, the appendix provides the

handbook-specified standards and foreign standards, international standards (ISD), and comparison and conversion of international unit systems (SI).

Chapter two compiles relatively completely the fundamental equations, key formulas, graphs and charts of airflow parameters in aerodynamics; equations of gas dynamics and thermodynamics; velocity potential equations, flow function equations, and characteristic curve equations commonly used in engineering; the relationship equations, graphs, charts, and flow elements among airflow parameters in various common situations.

Chapter three includes a chart on the standard atmosphere. The chart was compiled by systematic calculations based on specifications of the standard atmosphere and the practical requirements of aircraft. The altitude range of the atmosphere is 1000 meters to 32,000 meters with intervals of 50 to 100 meters. Moreover, there are tables of total pressure, total temperature and velocity pressure from altitude 0 to 32,000 meters and Mach number 0 to 3.6 with altitude interval of 1,000 meters, and interval for Mach number of 0.1, 0.2 and 0.05.

Volume Two   Calculation Methods of Longitudinal Direction Aerodynamic Characteristics in Static State

This volume presents calculation methods of longitudinal direction aerodynamic characteristics (in a static state) of a "clean" aircraft without objects attached to the fuselage exterior. The volume includes five parts: wing types, aircraft wings, fuselage, wing-fuselage combination, and wing-fuselage-tail combination. In addition, the aeroydnamic characteristics and forms of aerodynamic layout are presented as units with compilation in loose-leaf format. The part-by-part introduction is as follows:

Wing Types: This part (Part I) includes 21 loose leaves; main contents cover wing-type data, calculation methods of aerodynamic characteristics, and design methods of wing types.

11

Collection of wing-type data includes more than 200 wing types of the NACA series (which is used most extensively at present), five groups of the RAE series wing types with 4 to 5 percent relative thickness, and more than 20 wing types of the TsAGI series commonly used in Chinese aircraft. Also, some NLR research wing types by the Holland Aeronautical Research Institute are presented for checking the numerical calculation methods.

In the wing types of the NACA series, there are more than 20 fundamental mid-arc wing types of various groups, more than 90 low-speed fundamental thickness wing types (with relative thickness between 6 and 24 percent), and high-speed fundamental thickness wing types (with relative thickness between 2 and 21 percent), and more than 90 combination wing types in common use. More than 90 high-speed wing types (using the interpolation value) are presented. In addition to presenting geometric data and pressure distribution in the above wing types, force-measurement data of low-speed wind-tunnel tests of more than 200 wing types given by laboratories of various countries are presented.

Geometric data and pressure distribution data on TsAGI, RAE and NLR wing types are given.

In calculation of the aerodynamic characteristics of wing types, in addition to engineering methods, two pressure-distribution calculation methods of sub-critical winding flow are presented: the classic Xi'aodaosheng [transliteration] method and the source congruence method capable of calculating two-dimensional arbitrary wing types. In order to meet requirements satisfying the calculation of transonic winding flow, this part presents a method of conformal and cropping shear transformation for calculating pressure distribution of wing types; this method is adaptable to a blunt nose and thick wing with lift. In consideration of quick calculation in engineering practice, this part also uses the loosening method to conduct substitution of successive differences to solve the approximate velocity potential at sonic speed; this method is only limited to small angle-of-attack wing types with the nose not very thick. The calculation time is relatively short and its accuracy relatively high.

12

In the chapter on design data and method for wing types, large amounts of statistical data for the current aircraft are presented. In addition, combination and assembling technique for standard wing types are presented in detail. To provide convenience in designing wing types precisely, a two-stage approximate theoretical design method of a subcritical situation is given. By conforming to the method, wing types can be designed from given pressure distribution; the design method can be also used in composite design, in deriving the curvature distribution of wing types and parameters of the corresponding angle of attack from a given pressure distribution of the upper wing surface and thickness of wing types. For transonic wing types, this part presents an approximate method of engineering design. Based on the relationships among the given Mach number, pressure coefficients, and coordinates of circumference of wing surface, wings of exterior enclosed type with pressure distribution can be designed. As revealed by calculation examples, when M=0.75, errors of the chord direction and of the longitudinal-direction coordinates are, respectively, 0.6 and 0.7 percent.

Aircraft wings: Covering 19 loose leaves, this part (Part II) presents the calculation method of the aerodynamci characteristics of aircraft wings. In calculating characteristics of lift and dip moment, calculation methods are given for symmetrical wing types, and for ordinary plane-shape wings without torsion; the accuracy is no lower than the level currently among common data abroad. For supplements, the semi-empirical estimate method for a special situation is given. Moreover, this part presents the estimate method of the critical angle of attack and the maximum lift coefficient of aircraft wings from low speed to supersonic range. Compared to the experimental results, calculation errors of the maximum lift coefficient for wings of large and small aspect ratios do not exceed, respectively, 5 and 3 percent.

In calculation of the drag characteristics, this part presents calculation curves of cohesive drag and thick-wave drag; the calculation curves of drag-to-lift of ordinary plane-shape wings (without bending and/or torsion) in a subsonic state; and calculation curves of supersonic drag calculated with conic flow. In considering the requirement of utilizing results of wind-tunnel tests, this part presents a test revision method using the semi-empirical coefficient of drag to lift.

13

In order to calculate the aerodynamic characteristics of any plane shape, arbitrary cross section under bending and torsion, this part presents a program of numerical calculation of lift surface theory (fundamental solution) of a subsonic and supersonic thin wing. The calculation program can be used for wings with a straight line at the rear fringe and as many as three straight-line sectors at the front fringe of aircraft wings. After a wing is divided into 120 sectors, pressure distribution, lift, dip moment, and drag to lift can be relatively accurately calculated.

Fuselage: This part (Part III) mainly deals with the theory of a long slender body in a total of 17 loose leaves; calculation methods of fuselage aerodynamic characteristics are given with large amounts of test data. With this approach, calculation can be relatively accurate for regular-shaped fuselages. For fuselages with irregular configuration, this part recommends multiple methods of engineering treatment; in addition, a relatively rigorous program of numerical calculation is given.

At subsonic speed, the calculation method for deriving lift and dip moment can be used for a 12° to 16° angle of attack; the angle of attack adaptable to transonic and supersonic speeds is also greater.

Fuselage drag is calculated separately on different drag types. The frictional drag at the surface can be calculated by using the conventional method of an equivalent plate. The surface pressure drags (mainly of wave drags) are derived, respectively, on different nose shapes (tipped nose, slotted nose, and 30° truncated cone), tail shapes (cut tail and tipped tail), and nose exterior as an n-th power curve in order to comprise a set of data, including the set of data of the drag coefficient for the interference wave of the tail caused by the nose. For bottom drag of jet flow and wave drag of the cabin cover, this part also presents an estimate method for design and application.

In order to avoid errors in engineering estimates because of simplification of the fuselage, this part presents programs of numerical calculation of subsonic and supersonic lift and drag for a fuselage of arbitrary cross-section with

14

curvature and angle of attack. In order to provide the pressure gradient of a real fuselage during detailed design, the calculation method of fuselage pressure distribution in a subsonic and supersonic stream is also presented.

Combination: In all 22 loose leaves, this portion (Part IV and V) includes two parts: wing--fuselage and wing--fuselage--tail.

The aerodynamic characteristics of the wing--fuselage combination are mainly the calculation of interference factors. This part extends the interference factors currently only adaptable to a single midwing, cylindrical fuselage combination into a combination of bending-torsion wings. Moreover, the interference factor of an elliptical fuselage--single midwing combination is derived theoretically; moreover, the experimental verified revision factor is given. In addition, the part presents the trial method of estimating the interference factor of a non-single midwing--fuselage combination.

When dealing with the effect on the moment characteristic by down-wash flow of the wing-tip vortex system, this part presents subsonic and supersonic estimate methods, very close to test results. As verified by tests of multiple configurations, the interference [factor ? [shown in the next text page]] estimated with this method ....

15

curvature and angle of attack. In order to provide the pressure gradient of
a real fuselage during detailed design, the calculation method of fuselage
pressure distribution in a subsonic and supersonic stream is also presented.

Combination: In all 22 loose leaves, this portion (Part IV and V) includes
two parts: wing--fuselage and wing--fuselage--tail.

The aerodynamic characteristics of the wing--fuselage combination are
mainly the calculation of interference factors. This part extends the interference
factors currently only adaptable to a single midwing, cylindrical fuselage
combination into a combination of bending-torsion wings. Moreover, the inter-
ference factor of an elliptical fuselage--single midwing combination is derived
theoretically; moreover, the experimental verified revision factor is given. In
addition, the part presents the trial method of estimating the interference
factor of a non-single midwing--fuselage combination.

When dealing with the effect on the moment characteristic by down-wash flow
of the wing-tip vortex system, this part presents subsonic and supersonic estimate
methods, very close to test results. As verified by tests of multiple configura-
tions, the interference factor estimated with this method has, within the range
of a small angle of attack, a relative error of approximately 3 to 7 percent.
Generally, the error in inclination of the lift line is ± 3 percent, and the error
of focus is within the range of ± 5 percent. All these errors are less than that
calculated from the currently used methods.

The calculation of aerodynamic characteristics of the wing--fuselage--tail
combination is mainly derived from calculating the mutual interference among
various components, and then the contributions of individual components are
superimposed. Thusly, this part [of the handbook] presents the engineering
estimate method of down-wash flow of the wing--fuselage combination of
subsonic, transonic and supersonic velocities, as well as the engineering
estimate method of the velocity retarding coefficient (for a thick wing) of
the wake of the wing--fuselage combination. Compared with the experimental
results, the relative error of the engineering estimate method is within 10 and
7 percent. Derivations from the aforementioned calculations can lead to estimate
methods of pressure center and lift for a flat tail.

16

At the present time, a more rigorous estimate method for the drag characteristics of the wing--fuselage--tail combination is not available. Beginning from the elementary physics regime, this part presents a rough estimate of drag, as a preliminary estimate of the drag of the combination.